

Atmospheric-pressure plasma treatments applied on titanium dioxide layer for Sb₂S₃ solar cells applications

Tratamientos con plasmas a presión atmosféricos aplicados a la capa de dióxido de titanio para su aplicación en celdas solares de Sb₂S₃

HERNÁNDEZ-GRANADOS, Araceli^{1†*}, BECERRA-PANIAGUA, Dulce², MARTÍNEZ-VALENCIA, Horacio¹

¹Instituto de Ciencias Físicas, Universidad Nacional Autónoma de México, Av. Universidad 2001, Chamilpa 62210, Cuernavaca, Mexico

²Instituto de Energías Renovables, Universidad Nacional Autónoma de México, Priv. Xochicalco S/N 62580, Temixco Morelos, Mexico

ID 1st Author: Araceli, Hernández-Granados / ORC ID: 0000-0001-9439-5362, CVU CONACYT ID: 442077

ID 2nd Co-author: Dulce K., Becerra-Paniagua / ORC ID: 0000-0003-0471-7044, CVU CONACYT ID: 457428

ID 3rd Coauthor: Horacio, Martínez-Valencia / ORC ID: 0000-0002-0695-3457, CVU CONACYT ID: 6408

DOI: 10.35429/JSL.2021.25.8.16.24

Received July 30 2021; Accepted December 30, 2021

Abstract

This work presents the effect of atmospheric-pressure plasma (APP) treatment on mesoporous TiO₂ (mp-TiO₂) layers for antimony sulfide (Sb₂S₃) solar cells. For this work, it was prepared heterojunctions of antimony sulfide (Sb₂S₃) thin films solid solution as the absorbing materials and cadmium sulfide (CdS) as a sensitized layer deposited by the successive ionic layer adsorption and reaction (SILAR) technique, the Sb₂S₃ was obtained by chemical bath deposition (CBD). The photovoltaic characteristics of the solar cells with APP treatment showed a power conversion efficiency (PCE) of 0.54% to 1.04% with APP 0- and 60-seconds treatment, respectively.

Plasma treatment, Solar cells, Antimony sulfide

Resumen

Este trabajo presenta el efecto del tratamiento con plasma a presión atmosférica (APP) sobre películas mesoporosas de TiO₂ (TiO₂-mp) para celdas solares de sulfuro de antimonio (Sb₂S₃). Para este trabajo, se prepararon heterouniones de sulfuro de antimonio (Sb₂S₃) de solución sólida de películas delgadas como materiales absorbentes y sulfuro de cadmio (CdS) como capa sensibilizadora, la cual fue depositada por la técnica de adsorción y reacción de capas iónicas sucesivas (SILAR) y se depositó el Sb₂S₃ por la técnica de baño químico (BQ). Las características fotovoltáicas de las celdas con tratamiento APP mostraron una eficiencia de conversión de energía de 0,54% a 1,04% con tratamiento APP 0 y 60 segundos, respectivamente.

Tratamientos con plasma, Celdas solares, Sulfuro de antimonio

Citation: HERNÁNDEZ-GRANADOS, Araceli, BECERRA-PANIAGUA, Dulce, MARTÍNEZ-VALENCIA, Horacio. Atmospheric-pressure plasma treatments applied on titanium dioxide layer for Sb₂S₃ solar cells applications. Journal Simulation and Laboratory. 2021, 8-25: 16-24

*Correspondence to Author (email: aracelih@icf.unam.mx)

†Researcher contributing as first Author.

Introduction

The use of semiconductor chalcogenide materials have become an important field of research as alternative for photovoltaic applications (Buffiere, Dhawale, and El-Mellouhi 2019). They have suitable optical band gaps, and are non-toxic, earth abundant and low-cost materials. The band gaps of semiconductor materials oscillate between 1.10-1.55 eV, possess a large absorption coefficient, therefore they work as optimal materials for solar cells devices (Tao n.d.).

Researchers around the world have obtained interesting power conversion efficiencies (PCE's) from chalcogenide materials based solar cells, for example: 5.1% efficiency from a solar cell with copper tin sulfide (Cu_2SnS_3) (Chantana et al. 2020), 3-4% with copper antimony sulfide (CuSbS_2) (Edley et al. 2018), 6.4% with silver bismuth sulfide (AgBiS_2) (Burgués-Ceballos et al. 2020), 9.2% with antimony selenide (Sb_2Se_3) (Li et al. 2019), 7.5% with antimony sulfide (Sb_2S_3) (Choi et al. 2014), 6.2% (De Bray Sánchez, Nair, and Nair 2018) and 6.63% (Wu et al. 2019) from an antimony sulfide selenide [$\text{Sb}_2(\text{S}_x\text{Se}_{1-x})_3$] solar cell.

Specially, the Sb_2S_3 thin films have received greater attention for their suitable properties for solar cell applications. For example, the antimony sulfide (Sb_2S_3) has a direct band gap of 1.70-1.88 eV, an orthorhombic crystal structure, a n-type conductivity, a hall mobility of $9.8 \text{ cm}^2\text{V}^{-1}\text{s}^{-1}$, a carrier concentration of $1.2 \times 10^{12} \text{ cm}^{-3}$, a high absorption coefficient ($>10^4 \text{ cm}^{-1}$), and a resistivity of $5.3 \times 10^6 \text{ ohm.cm}$ (X. Wang et al. 2018), (Ben Nasr et al. 2011), (Kondrotas, Chen, and Tang 2018), when it is prepared by chemical bath deposition (CBD).

For this reason, different types of configurations have been used to obtain better PV properties. For example, it is widely studied the use of metal oxides such as TiO_2 , due to it is a versatile material useful for photocatalysis, hydrogen generation and solar energy application. A typical solar cell configuration has a blocking layer of titanium dioxide (TiO_2), a mesoporous layer of TiO_2 , an absorbing material or generator of electron-hole carriers and back contacts of carbon or silver.

In the case of the mesoporous TiO_2 film, it is considered crucial for optimal performance, because it provides a greater surface area, minimizes the migration of photogenerated electrons between the semiconductor and the electron transport layer, which helps to decrease exciton recombination, in addition the thickness and morphology affect the optical and electrical properties of the device in general.

Therefore several efforts have led to modify characteristic on the materials in order to increase the efficiency of solar cells, such as plasma^{13,14}, sulfurization (Guo et al. 2019), (B. Yang et al. 2017), selenization (Yuan et al. 2017), (Zhang et al. 2017), post annealing (X. Wang et al. 2017), thioacetamide (TA)-based sulfurization (Choi et al. 2014) and plasma treatments (Calixto-Rodriguez et al. 2010), to mention a few. The plasma treatment can modify the wettability of materials due to the interactions of free radicals (Domínguez-Díaz, Escorcia-García, and Martínez 2019), (Nishihara et al. 2018), degradation of textile dyes (Vergara Sanchez et al. 2017), improve PV characteristic such as: conductivity, mobility (Y. Wang et al. 2019), low-density of defect state (K. Wang et al. 2019) and in consequence the increase of the PCE. Most of these treatments shown a mixture of nitrogen/oxygen, CO_2 , argon/oxygen or just argon.

In this work, we report an atmospheric-pressure plasma (APP) treatment on mesoporous titanium dioxide (mp- TiO_2), used as part of window layers for antimony sulfide (Sb_2S_3) solar cells (SC's). It is demonstrated that APP treatment can modify optical and structural properties of mp- TiO_2 and improve photovoltaic performance of the corresponding solar cells.

Methodology

As part of the configuration's solar cells of Sb_2S_3 based on TiO_2 -mesoporous, different materials were deposited as follow: compact TiO_2 (bl- TiO_2), mesoporous TiO_2 (mp- TiO_2), cadmium sulfide (CdS), antimony sulfide (Sb_2S_3) and silver contacts.

– Blocking TiO_2

First, a 30 nm blocking TiO_2 layers (bl- TiO_2) were deposited on cleaned FTO-coated glass substrates. All the process is summarized in Figure 1.

Materials

- Titanium tetraisopropoxide (TTIP, Ti [OCH (CH₃)₂]₄, Sigma Aldrich, 97%)
- 2-propanol (CH₃CH (OH) CH₃, J.T. Baker, 99.9%)
- Hydrochloric acid (HCl, J.T. Baker, 36.5-38%)

A 20 mL of 2-propanol were added, then 1.2 mL of titanium tetraisopropoxide and 0.4 mL of HCl were slowly added. The solution obtained was kept stirring at 450 rpm for 30 minutes. As a result, a clear-yellow solution was obtained. This solution was deposited by spin coating. The spin coating process consisted of using a FTO substrate and the TiO₂ precursor solution was added. Finally, the bl-TiO₂ layers were treated at 450 °C for 30 minutes (Hernández-Granados et al. 2016).

– Mesoporous TiO₂

To obtain the mesoporous titanium dioxide (mp-TiO₂) precursor solution, the materials used are listed below:

Materials

- Titanium tetraisopropoxide (TTIP), Ti [OCH (CH₃)₂]₄, (Sigma Aldrich, 97%)
- Poly (vinylpyrrolidone) (PVP, Mw ~ 1,300,000, Sigma Aldrich)
- Ethanol (CH₂H₆O, J.T. Baker, 99.9%)
- Hydrochloric acid (HCl, J.T. Baker, 36.5-38%)
- Acetic acid (CH₃COOH, Fermont, 99.9%)

The precursor solution of mp-TiO₂ was prepared by the synthesis of two different solutions labeled as A and B. The first solution A: 7.5 ml of ethanol and 0.45 grams of PVP stirring at 900 rpm for 15 minutes. The solution B: 3 ml of ethanol, 3 ml of acetic acid, 1.5 ml of Ti tetraisopropoxide keeping the stirring at 900 rpm for 15 minutes. Then the solution B was added on solution A and was stirred at 900 rpm for 1 hour. After this, a 0.5 ml of the precursor solution was deposited on bl-TiO₂ by spin coating and the samples were thermally treated at 550 °C for three hours.

– Atmospheric-pressure plasma treatments

After that, atmospheric-pressure plasma (APP) treatments were done on the surface of the mp-TiO₂ layers. The distance between the electrode and the sample was 3 cm. APP treatments were applied for 0, 15, 30 and 60 seconds in each sample.

– Cadmium sulfide

The mp-TiO₂ layers were sensitized by cadmium sulfide (CdS) with the SILAR technique, which consists of having the anion and the cation in separate solutions.

Materials

- Cadmium chloride (CdCl₂, J.T. Baker, 79.9%)
- Sodium sulfide (Na₂S, Fermont, 99.6%)
- Methanol (CH₃OH, J.T. Baker)

For this purpose, separate solutions were prepared at 0.05 M of cadmium chloride and sodium sulfide, used as precursors of cadmium and sulfide respectively. The solutions were prepared as 50:50 ratios of distilled water and methanol. The deposition technique consisted of immersing the previously obtained substrate in the cadmium chloride solution for 60 s, at the end of 60 s, the substrate was placed in a solution of 50:50 distilled water and methanol for 30 s to remove the excess material from the previous dipping in CdCl₂, then the substrate was immersed in the sodium sulfide solution for 60 s and finally it was again immersed in a 50:50 solution of distilled water and methanol as a final wash and to remove excess Na₂S. This entire process was called a SILAR cycle. For the present work, 25 cycles were carried out.

– Sb₂S₃ solar cells preparation

The deposition of Sb₂S₃ was carried out by chemical bath deposition (CBD). The chemical solution was constituted by 20 ml of 0.1 M potassium antimony tartrate, 20 ml of 1 M tartaric acid, 31 ml of distilled water, 6 ml of 7 M ammonium hydroxide, and 3 ml of 0.2 M sodium selenosulfate. The solution had a pH of 10. The FTO/bl-TiO₂/mp-TiO₂/CdS samples were immersed in that chemical bath at 80 °C for 1.5 h, obtaining in ~120 nm thick Sb₂S₃ films.

Then they were annealed at 270 °C in nitrogen for 30 min at 1 atm to become crystalline Sb_2S_3 (Ayala-Sánchez, Escorcia-García, and Alonso-Lemus 2020; Escorcia-García et al. 2018). To complete the PV devices, graphite contacts (0.25 cm^2) were placed on top of the absorber (Sb_2S_3).

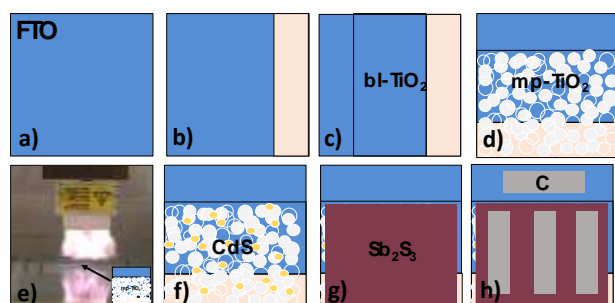


Figure 1 Fabrication process of the two types of solar cells: a) Fluorine doped Tin Oxide (FTO) glass, b) etching of the FTO, c) deposition of the blocking TiO_2 layer by spin-coating, d) deposition by spin-coating of the mesoporous TiO_2 , e) atmospheric plasma treatment on the surface of mp-TiO_2 , f) deposition of the CdS by SILAR technique, g) Sb_2S_3 deposition by chemical bath deposition and h) contacts.

Table 1 shows all the configuration details for the solar cells prepared of this work.

Label	Configuration	APP time
A	$\text{bl-TiO}_2/\text{mp-TiO}_2$	0
B	$\text{FTO/bl-TiO}_2/\text{mp-TiO}_2/\text{Sb}_2\text{S}_3/\text{C}$	0
C	$\text{FTO/bl-TiO}_2/\text{mp-TiO}_2(\text{APP-0})/\text{CdS}/\text{Sb}_2\text{S}_3/\text{C}$	0
D	$\text{FTO/bl-TiO}_2/\text{mp-TiO}_2(\text{APP-15})/\text{CdS}/\text{Sb}_2\text{S}_3/\text{C}$	15 s
E	$\text{FTO/bl-TiO}_2/\text{mp-TiO}_2(\text{APP-30})/\text{CdS}/\text{Sb}_2\text{S}_3/\text{C}$	30 s
F	$\text{FTO/bl-TiO}_2/\text{mp-TiO}_2(\text{APP-60})/\text{CdS}/\text{Sb}_2\text{S}_3/\text{C}$	60 s

Table 1 Configuration details of the PV devices

Characterization

The film thickness was measured using a profilometer (Ambios technology XP-200). Optical transmission (T) and reflection (R) spectra of thin film samples were measured using a UV-Vis-NIR spectrophotometer (Jasco V-670). An atmospheric plasma from Diener Electronic GmbH+Co., KG model APC500 Spray Corona) with a line of air at atmospheric pressure, and a power generator capable of producing approximately 500 W at a voltage of 10 kV and at a gas pressure of 1500 Torr.

Raman spectra were measured using a Raman SENTERRA II (Bruker), Olympus microscope (20X objective), software OPUS 7.8, laser with a wavelength of 785 nm and power of 10 mW, 2 scans were acquired for each spectrum, each with an integration time of 60,000 ms. The I-V curves of solar cells were obtained with a Keithley 230 programmable voltage supply coupled with a Keithley 619 multimeter under a 400 W/m^2 radiation intensity from a white-light LED. I

Results and discussion

In this section it is presented the solar cells obtained by chemical bath of Sb_2S_3 used as absorber semiconductor supported on mesoporous titanium dioxide (mp-TiO_2), as well as the use of a CdS sensitizing. The results are divided in two sections: optical and photovoltaic.

– Optical

Figure 2, shows digital photographs from the obtained solar with $\text{bl-TiO}_2/\text{mp-TiO}_2/\text{CdS}/\text{Sb}_2\text{S}_3$: a) solar cell without CdS , in this image it is clear to see the low deposit rate of Sb_2S_3 on the surface of mp-TiO_2 , b) this solar cell has a yellow-brown color, which results from the combination of CdS and Sb_2S_3 , without any APP treatment, c) and d) these solar cells show a homogeneous deposit and a darker color, due to the increase in thickness and APP treatment of 15 and 30 s, respectively, and e) solar cell with APP of 60 s, shows a darker color due to the increase of thickness of Sb_2S_3 .



Figure 2 Digital images: a) $\text{bl-TiO}_2/\text{mp-TiO}_2$, b) $\text{bl-TiO}_2/\text{mp-TiO}_2(\text{P0})/\text{CdS}(25)/\text{Sb}_2\text{S}_3$, c) $\text{bl-TiO}_2/\text{mp-TiO}_2(\text{P15})/\text{CdS}(25)/\text{Sb}_2\text{S}_3$, d) $\text{bl-TiO}_2/\text{mp-TiO}_2(\text{P30})/\text{CdS}(25)/\text{Sb}_2\text{S}_3$ and e) $\text{bl-TiO}_2/\text{mp-TiO}_2(\text{P60})/\text{CdS}(25)/\text{Sb}_2\text{S}_3$.

Figure 3 shows the surface images of mp-TiO_2 taken by Raman SENTERRA II Bruker, Olympus microscope, software OPUS 7.8. Figures a) and b) are deposited on glass with 0 and 120 s of APP treatment, in comparison the sample b shows a homogenous morphology and smaller grains when the APP is applied; figure c) and d) are samples deposited on FTO substrates with 30 and 120 s, respectively.

In comparison the morphology changes drastically when the time is 3 times longer; showing a homogenous deposit after applying 120 s of APP.

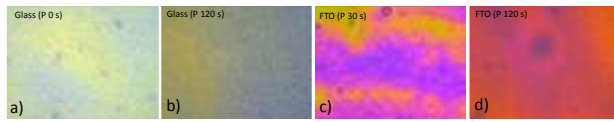


Figure 3 Surfaces images a) mp-TiO₂ on glass substrate at 0 s of plasma treatment, b) mp-TiO₂ on glass substrate at 120 s of plasma treatment, c) mp-TiO₂ on FTO substrate at 30 s of plasma treatment and d) mp-TiO₂ on FTO substrate at 120 s of plasma treatment

The UV-Vis-NIR characterization was performed to study the changes of transmittance (T) and reflectance (R) because of APP. In figure 4, it is showing the blocking and mesoporous TiO₂ layers with APP treatments at 0, 15, 30 and 60 s. Black line belongs to bl-TiO₂ film, it shows a uniform spectrum in T and R measurements. The film labeled as bl-TiO₂/mp-TiO₂ shows a typical TiO₂ absorption (380 nm) and some waves on the spectrum, this is related to the effect of light dispersion due to the porous structure (blue line).

The samples with APP treatment at 15, 30 y 60 seconds (green, wine and orange lines, respectively) showed an increase of T (from 60 to 70%) at 400 nm and R at 450 nm compared with the pristine film. This might be attributed to the detachment of TiO₂ material at the time of the APP process, thus the thickness is reduced. As the CdS is deposited onto the films (thinner lines), the light absorption moves to the visible range, because of the effect of the new material incorporation and its different band gap (2.5 eV)(Mukherjee et al. 2015).

The final structure it is not completely covered by the CdS due to the synthesis type used (SILAR). With this method is possible to form dots and sensitized the surface of mp-TiO₂, therefore the mp-TiO₂ contribution spectrum remains even with the CdS deposition.

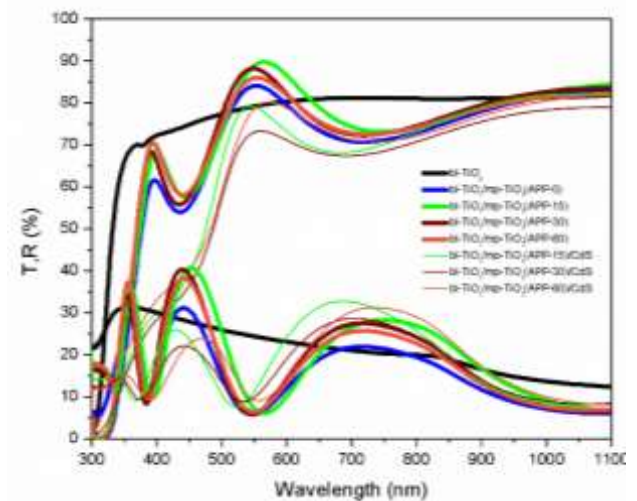


Figure 4 Optical measurements: Transmittance and reflectance of mp-TiO₂ with APP and CdS as sensitizer.

Raman analysis is very sensitive characterization technique, and it was carried out to identify structural properties and understand the modification of TiO₂ with and without the APP treatment. Figure 5 shows the complete Raman spectrum measured from 0-3000 cm⁻¹ and the difference in intensity between the sample APP-0 and the other samples. At the region of 0-1000 cm⁻¹, shows the vibrational modes between 100-900 cm⁻¹, related to characteristic peaks of Anatase phase TiO₂ according to previous works (Ekoi et al. 2019).

Also, it is possible to see a peak around 1374 cm⁻¹ corresponding to the C-H₂ bending observed in pure PVP (Zidan et al. 2019), while the band at 1800-1900 cm⁻¹ is related to carbonyl compounds, caused by the stretching of the C=O bond (L. Yang, Wu, and Zhao 2015) (Colthup, Daly, and Wiberley 1990).

The notably decrease of peak intensities in 1000-2000 cm⁻¹ region after APP treatment suggests the reduction of PVP traces at the surface of mp-TiO₂, as it was reported by our group before (Hernández-Granados et al. 2019). This can be related to the oxide's crystallinity from the temperature used (Yan et al. 2013) in the plasma treatments.

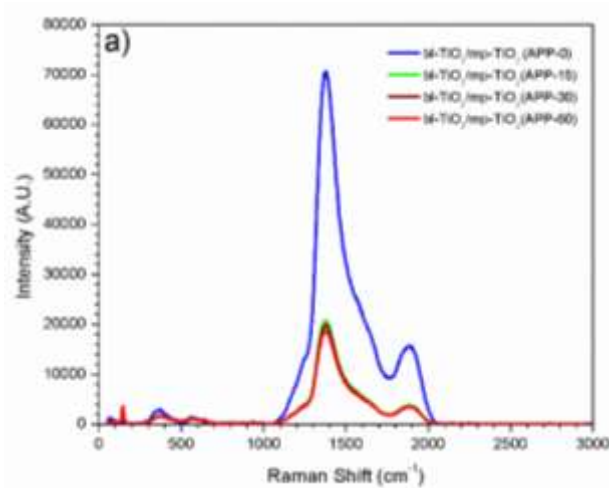


Figure 5 Raman spectra of TiO₂ at different APP: a) region of 0-3000 cm⁻¹, b) region of 0-1000 cm⁻¹

PV performance

To understand the effect of APP on PV devices, the current density-voltage (J-V) curves of solar cells were acquired under AM 1.5 irradiation treated with different times of APP. Figure 6 shows J-V curves of the configuration FTO/bl-TiO₂/mp-TiO₂(APP)/CdS/Sb₂S₃/C. The lowest PV parameters are from the solar cell without any APP or CdS treatment: open-circuit voltage (V_{oc}) = 420 mV, short-circuit current density (J_{sc}) = 0.74 mA/cm², fill factor (FF) = 0.33 and power conversion efficiency (PCE) = 0.26%.

However, when the CdS is included, it is observed that V_{oc} and J_{sc} increased, giving better PV parameters and by doing that the PCE increased by double (V_{oc} = 550 mV, J_{sc} = 2.06 mA/cm², FF = 0.19, and PCE = 0.54%). With the APP treatment on mp-TiO₂ layers, the photovoltaic performance is improved even more.

The main increases are observed in V_{oc} and FF; the APP-15, APP-30 and APP-60 showed V_{oc} of 590, 540, and 570 mV, and FF of 0.18, 0.26 and 0.41, giving improved PCE values of 0.58%, 0.55% and 1.04%, respectively. Table 2 summarizes PV parameters for all the solar cell samples showed in Figure 6.

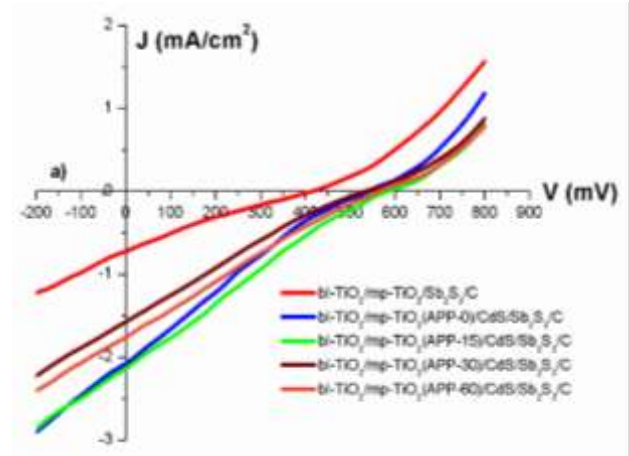


Figure 6 J-V of Sb₂S₃ solar cells under AM1.5 irradiation treated with different times of APP treatment

Sample	V_{oc} (mV)	J_{sc} (mA/cm ²)	FF	PCE (%)
FTO/bl-TiO ₂ /mp-TiO ₂ /Sb ₂ S ₃ /C	420	0.74	0.33	0.26%
FTO/bl-TiO ₂ /mp-TiO ₂ (APP-0)/CdS/Sb ₂ S ₃ /C	550	2.06	0.19	0.54%
FTO/bl-TiO ₂ /mp-TiO ₂ (APP-15)/CdS/Sb ₂ S ₃ /C	590	2.13	0.18	0.58%
FTO/bl-TiO ₂ /mp-TiO ₂ (APP-30)/CdS/Sb ₂ S ₃ /C	540	1.57	0.26	0.55%
FTO/bl-TiO ₂ /mp-TiO ₂ (APP-60)/CdS/Sb ₂ S ₃ /C	570	1.77	0.41	1.04%

Table 2 Photovoltaic parameters obtained from J-V curves in figure 6

Thanks

The authors gratefully acknowledge the graduate students Norah Rebolledo (ICF-UNAM) & Fabián Arias (IER-UNAM) for the supportive help in the laboratories. AHG thanks CONACYT for her postdoctoral scholarship.

Conclusions

The mesoporous TiO₂ layers were obtained by simple sol-gel synthesis and the incorporation of Sb₂S₃ for solar cells was successfully carried out with CBD methods. It was presented the contribution of the CdS by SILAR technique as the light absorption moved to the visible range, because of the effect of the new material incorporation and its different band gap. The air pressure plasma (APP) treatment can modify the surface and optical properties of sol-gel prepared the mesoporous TiO₂ thin film layers.

The Raman analysis confirms the Anatase phase in mp-TiO₂ samples. It also shows that the intensities of those peaks related to the C-H₂ and stretching of the C=O bond, originated from the surfactant trace (PVP) and they are significantly reduced in mp-TiO₂ samples after APP treatment. Finally, photovoltaic performance of Sb₂S₃ based solar cells is improved when the APP treatment was done for 60 seconds on mp-TiO₂ layers, obtaining 1.04% of power conversion efficiency. APP treatment is a useful method to modify surface chemistry and structure of semiconductor thin films.

References

- Ayala-Sánchez, M.I., J. Escorcia-García, and I.L. Alonso-Lemus. 2020. "Effect of Sb Doping and Polyvinylpyrrolidone on the Mesoporous TiO₂ Photoanodes for Sb₂Se₃ Sensitized Solar Cells." *MRS Advances*: 1–10.
- De Bray Sánchez, Fabiola, M. T.S. Nair, and P. K. Nair. 2018. "Optimum Chemical Composition of Antimony Sulfide Selenide for Thin Film Solar Cells." *Applied Surface Science* 454(March): 305–12.
- Buffiere, Marie, Dattatray S. Dhawale, and Fedwa El-Mellouhi. 2019. "Chalcogenide Materials and Derivatives for Photovoltaic Applications." *Energy Technology* 7(11): 1–17.
- Burgués-Ceballos, Ignasi, Yongjie Wang, M. Zafer Akgul, and Gerasimos Konstantatos. 2020. "Colloidal AgBiS₂ Nanocrystals with Reduced Recombination Yield 6.4% Power Conversion Efficiency in Solution-Processed Solar Cells." *Nano Energy* 75: 104961.
- Calixto-Rodríguez, M. et al. 2010. "A Comparative Study of the Physical Properties of Sb₂S₃ Thin Films Treated with N₂ AC Plasma and Thermal Annealing in N₂." *Applied Surface Science* 256(8): 2428–33.
- Chantana, Jakapan et al. 2020. "Investigation of Carrier Recombination of Na-Doped Cu₂SnS₃ Solar Cell for Its Improved Conversion Efficiency of 5.1%." *Solar Energy Materials and Solar Cells* 206(September 2019): 110261. <https://doi.org/10.1016/j.solmat.2019.110261>.
- Choi, Yong Chan et al. 2014. "Highly Improved Sb₂S₃ Sensitized-Inorganic-Organic Heterojunction Solar Cells and Quantification of Traps by Deep-Level Transient Spectroscopy." *Advanced Functional Materials* 24(23): 3587–92.
- Colthup, Norman B., Lawrence H. Daly, and Stephen E. Wiberley. 1990. "CARBONYL COMPOUNDS." In *Introduction to Infrared and Raman Spectroscopy*, Elsevier, 289–325.
- Domínguez-Díaz, Maraolina, José Escorcia-García, and Horacio Martínez. 2019. "Influence of the Crystalline Structure Stability in the Wettability of Poly-β-Hydroxybutyrate:Polyethylene Glycol 6000 Fiber Mats Treated by Atmospheric-Pressure Plasma." *Nuclear Instruments and Methods in Physics Research, Section B: Beam Interactions with Materials and Atoms* 447(August 2018): 84–91. <https://doi.org/10.1016/j.nimb.2019.03.041>.
- Edley, Michael E. et al. 2018. "Solution Processed CuSbS₂ Films for Solar Cell Applications." *Thin Solid Films* 646(December 2017): 180–89. <https://doi.org/10.1016/j.tsf.2017.12.002>.
- Ekoi, E. J., A. Gowen, R. Dorrepaal, and D. P. Dowling. 2019. "Characterisation of Titanium Oxide Layers Using Raman Spectroscopy and Optical Profilometry: Influence of Oxide Properties." *Results in Physics* 12(December 2018): 1574–85. <https://doi.org/10.1016/j.rinp.2019.01.054>.
- Escorcia-García, J., M. Domínguez-Díaz, A. Hernández-Granados, and H. Martínez. 2018. "Antimony Sulfide Thin Films Obtained by Chemical Bath Deposition Using Tartaric Acid as Complexing Agent." *MRS Advances* 3(56): 3307–13.
- Guo, Liping et al. 2019. "Scalable and Efficient Sb₂S₃ Thin-Film Solar Cells Fabricated by Close Space Sublimation." *APL Materials* 7(4). <http://dx.doi.org/10.1063/1.5090773>.
- Hernández-Granados, Araceli et al. 2016. "Sb₂(S_xSe_{1-x})₃ Sensitized Solar Cells Prepared by Solution Deposition Methods." *Materials Science in Semiconductor Processing* 56: 222–27. <http://dx.doi.org/10.1016/j.mssp.2016.08.022>.

- Hernández-Granados, Araceli et al. 2019. "Optically Uniform Thin Films of Mesoporous TiO₂ for Perovskite Solar Cell Applications." *Optical Materials* 88(December 2018): 695–703.
- Kondrotas, Rokas, Chao Chen, and Jiang Tang. 2018. "Sb₂S₃ Solar Cells." *Joule* 2(5): 857–78. <https://doi.org/10.1016/j.joule.2018.04.003>.
- Li, Zhiqiang et al. 2019. "9.2%-Efficient Core-Shell Structured Antimony Selenide Nanorod Array Solar Cells." *Nature Communications* 10(1): 1–9. <http://dx.doi.org/10.1038/s41467-018-07903-6>.
- Mukherjee, A. et al. 2015. "Synthesis of Nanocrystalline CdS Thin Film by SILAR and Their Characterization." *Physica E: Low-Dimensional Systems and Nanostructures* 65: 51–55. <http://dx.doi.org/10.1016/j.physe.2014.08.013>.
- Ben Nasr, T., H. Maghraoui-Meherzi, H. Ben Abdallah, and R. Bennaceur. 2011. "Electronic Structure and Optical Properties of Sb₂S₃ Crystal." *Physica B: Condensed Matter* 406(2): 287–92. <http://dx.doi.org/10.1016/j.physb.2010.10.070>.
- Nishihara, Yoshihiko et al. 2018. "Influence of O₂ Plasma Treatment on NiO_x Layer in Perovskite Solar Cells." *Japanese Journal of Applied Physics* 57(4): 2–6.
- Tao, Meng. *SPRINGER BRIEFS IN APPLIED SCIENCES AND TECHNOLOGY Terawatt Solar Photovoltaics Roadblocks and Opportunities*. <http://www.springer.com/series/8884>.
- Vergara Sanchez, Josefina et al. 2017. "Degradation of Textile Dye AB 52 in an Aqueous Solution by Applying a Plasma at Atmospheric Pressure." *IEEE Transactions on Plasma Science* 45(3): 479–84.
- Wang, Kang et al. 2019. "Oxidation, Reduction, and Inert Gases Plasma-Modified Defects in TiO₂ as Electron Transport Layer for Planar Perovskite Solar Cells." *Journal of CO₂ Utilization* 32(March): 46–52. <https://doi.org/10.1016/j.jcou.2019.04.001>.
- Wang, Xiaomin et al. 2017. "A Fast Chemical Approach towards Sb₂S₃ Film with a Large Grain Size for High-Performance Planar Heterojunction Solar Cells." *Nanoscale* 9(10): 3386–90.
- Wang, Xiaomin et al. 2018. "Development of Antimony Sulfide–Selenide Sb₂(S, Se)₃-Based Solar Cells." *Journal of Energy Chemistry* 27(3): 713–21. <https://doi.org/10.1016/j.jechem.2017.09.031>.
- Wang, Yumeng, Hao Qu, Chunmei Zhang, and Qiang Chen. 2019. "Rapid Oxidation of the Hole Transport Layer in Perovskite Solar Cells by A Low-Temperature Plasma." *Scientific Reports* 9(1): 1–9. <http://dx.doi.org/10.1038/s41598-018-36685-6>.
- Wu, Chunyan et al. 2019. "Interfacial Engineering by Indium-Doped CdS for High Efficiency Solution Processed Sb₂(S_{1-x}Se_x)₃ Solar Cells." *ACS Applied Materials and Interfaces* 11(3): 3207–13.
- Yan, Junqing et al. 2013. "Understanding the Effect of Surface/Bulk Defects on the Photocatalytic Activity of TiO₂: Anatase versus Rutile." *Physical Chemistry Chemical Physics* 15(26): 10978–88.
- Yang, Bo et al. 2017. "In Situ Sulfurization to Generate Sb₂(Se_{1-x}S_x)₃ Alloyed Films and Their Application for Photovoltaics." 2(September 2016): 113–22.
- Yang, Linzhi, Wenpeng Wu, and Yi Zhao. 2015. "Effect of TiO₂ Particles on Normal and Resonance Raman Spectra of Coumarin 343: A Theoretical Investigation." *Physical Chemistry Chemical Physics* 17(16): 10910–18. <http://dx.doi.org/10.1039/C4CP05794E>.
- Yuan, Shengjie et al. 2017. "Postsurface Selenization for High Performance Sb₂S₃ Planar Thin Film Solar Cells." *ACS Photonics* 4(11): 2862–70. <https://pubs.acs.org/doi/abs/10.1021/acsp Photonics.7b00858> (June 28, 2020).
- Zhang, Yan et al. 2017. "Selenium-Graded Sb₂(S_{1-x}Se_x)₃ for Planar Heterojunction Solar Cell Delivering a Certified Power Conversion Efficiency of 5.71%." *Solar RRL* 1(5).

Zidan, Hamdy M., Elmetwally M. Abdelrazek, Amr M. Abdelghany, and Ahmed E. Tarabiah. 2019. "Characterization and Some Physical Studies of PVA/PVP Filled with MWCNTs." *Journal of Materials Research and Technology* 8(1): 904–13. <https://doi.org/10.1016/j.jmrt.2018.04.023>.